ACS APPLIED MATERIALS & INTERFACES

Research Article

www.acsami.org

Facile Approach to Preparing Microporous Organic Polymers through Benzoin Condensation

Yan-Chao Zhao,[†,‡] Tao Wang,[†] Li-Min Zhang,[†] Yi Cui,[†,‡] and Bao-Hang Han*[,†]

[†]National Center for Nanoscience and Technology, Beijing 100190, China

[‡]University of Chinese Academy of Sciences, Beijing 100049, China

Supporting Information

ABSTRACT: A series of microporous organic networks linked by α-hydroxyl ketone were synthesized based on benzoin self-condensation of multiformyl-containing building blocks. Fourier transform infrared and solid-state ^{13}C CP/MAS NMR spectroscopy were utilized to confirm the α-hydroxyl ketone linkage of the obtained polymers. The hollow microspheric morphology can be observed from scanning electron microscopy and transmission electron microscopy images. The materials, with Brunauer–Emmet–Teller specific surface area up to 736 $m^2\ g^{-1}$, possess a hydrogen storage capacity up to 1.42 wt % at 77 K and 1.0 bar and a carbon dioxide uptake up to 15.3 wt % at 273 K and 1.0 bar. These excellent characteristics would make them become promising candidates for gas storage.

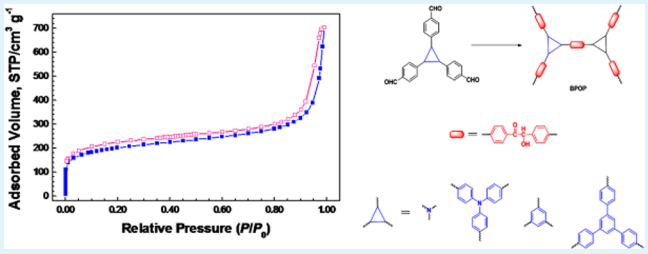

KEYWORDS: *microporous organic networks, benzoin self-condensation, α-hydroxyl ketone, BET specific surface area, hydrogen storage, carbon dioxide uptake*

INTRODUCTION

Microporous organic polymers have attracted intense interest because of their excellent potential as heterogeneous catalysts,[1] gas permeable membranes,[2] and light-emitting organics.[3] Over the past few years, considerable researches have been devoted to the preparation of various microporous organic polymers.[4,5] Mckeown and Budd reviewed recent progress in constructing of polymeric networks that possess intrinsic microporosity.[6] Many reactions employed and rigid monomers used to form rigid linkages to design microporous polymers were systemically summarized. Especially, the Mckeown group reported the formation of polymers of intrinsic microporosity (PIMs) based on the dioxane linkage between catechol and 1,2-difluoro-aryl units.[7] Conjugated microporous polymers and porous aromatic frameworks are also a huge family of microporous amorphous networks, which are assembled by noble metal-mediated ethynyl,[8] Sonogashira–Hagihara,[9] Suzuki,[3] and Yamamoto coupling reaction.[10] However, crystalline nanoporous polymers (i.e., covalent organic frameworks[11] and covalent triazine-based framework[12]) represent the most ordered porous structure for a given monomer through thermodynamically reversible condensation.

There are two general strategies for the preparation of porous organic polymers with high specific surface area and desirable functional moieties: (i) The design of rigid monomers, at least one of which contains a "site of contortion" and the average functionality of greater than two, should be considered.[2] Therefore, some nonplanar skeletons, such as tetraphenylethylene,[13] hexaphenylbenzene,[14] binaphthol,[15] tribenzotriquinacene,[16] and triptycene-substituted phthalocyanine,[17] were recently employed to prepare microporous polymers. Although the obtained polymers possess high specific surface area and nice gas storage capacity, the synthesis of monomers seems to be more complicated and time-consuming. Furthermore, not all rigid monomers obtained are effective to construct nanoporous materials, so it is also an important issue to search for the appropriate and interesting ones. (ii) The development of novel condensation reaction is an alternative choice to design microporous organic polymers. Many researchers have dedicated much effort into searching for new reaction starting with cheap and easily obtained monomers. Thus Schiff base chemistry between multiamino and multiformyl compounds,[18] aldol self-condensation of aromatic acetyl compounds,[19] hydrazone-forming reaction by condensation of phenylhydrazide with multiformyl compounds,[20] borazine-forming reaction between multiamino compounds and boron trihalides,[21] benzimidazole-forming reaction between *o*-phenylenediamine or bisquinone and multiformyl compounds,[22,23] Friedel–Crafts reaction between aromatic compounds and formaldehyde dimethyl acetal,[24] and oxidative coupling polymerization of multicarbazolyl monomers[25] were utilized to synthesize porous polymers. The different linkages between monomers can also provide different functional possibilities, which would somewhat expand the scope of applications. Thus, a facile and effective condensation shows a very important practical value.

Received: September 30, 2012
Accepted: November 30, 2012
Published: November 30, 2012

Scheme 1. Schematic Representation of Benzoin Condensation of Benzaldehyde

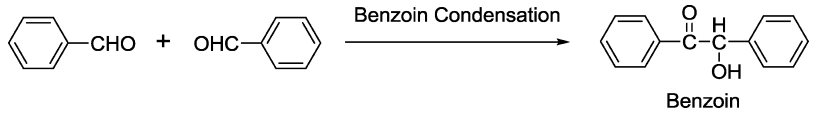

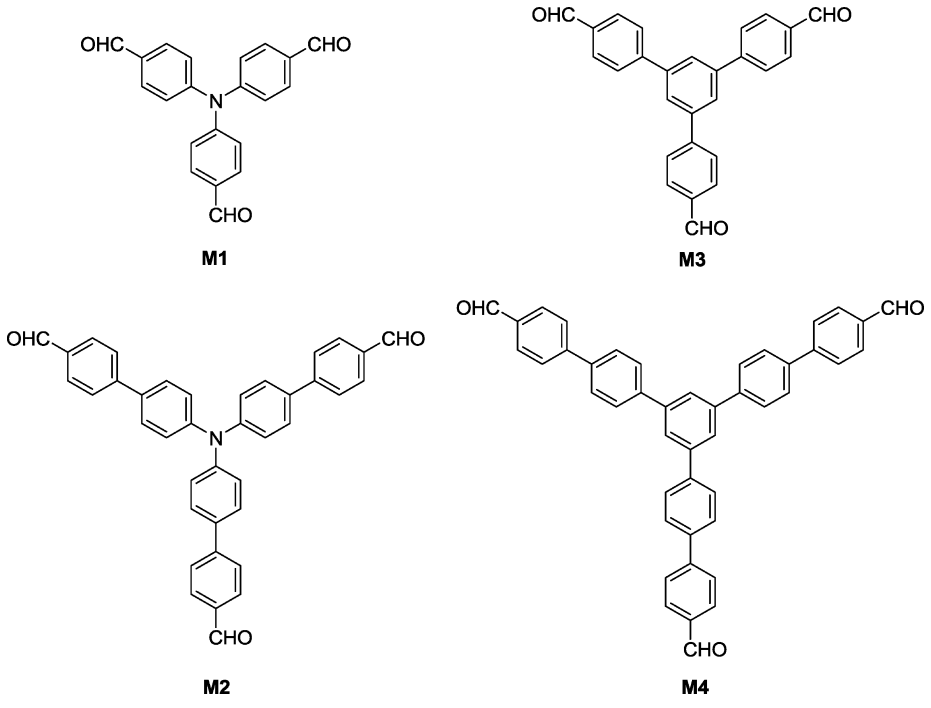

Figure 1. Structures of formyl-containing building blocks (**M1**–**M4**) used to prepare microporous organic polymers.

Although great achievements in synthesizing microporous organic polymers have been realized,[26] extremely high Brunauer–Emmet–Teller specific surface areas as high as 6461 m^2 g^{-1},[27] the other pore parameters, such as pore size, pore volume, and pore size distribution, are important in determining the gas sorption performance. Moreover, it is also a great challenge to search for a novel condensation reaction employed in the preparation of porous materials. Benzoin condensation might be an alternative choice. It is well-known that, with the assistance of acid catalyst, bimolecular condensation of benzaldehyde can yield an α-hydroxyl ketone structure (benzoin), and such a reaction can occur for many aromatic aldehydes (Scheme 1). Benzoin condensation fulfils the atom-economical principle, and no byproducts would be generated. This kind of reaction has been extensively applied in the organic synthesis.[28] However, to the best of our knowledge, employing multiformyl-containing compounds for the preparation of microporous polymers for gas storage remains unprecedented through benzoin condensation. Although various kinds of reactions with atom-economical principle to the preparation of microporous organic materials have been reported such as ethynyl cyclotrimerization,[29,30] click chemistry,[31] and cyano cyclotrimerization,[32,33] it is inevitable to use noble and/or transition metal (cobalt, copper, and zinc) catalysts in the whole process. In this paper, we employ a *p*-toluene sulfonic acid-catalyzed route to prepare microporous organic polymers with a high specific surface area through benzoin condensation. This easily processing procedure is a metal-free method, and the catalyst can be easily removed by washing with water and ethanol. Moreover, the formation of high-surface-area materials from cheap multiformyl-containing precursors is always of importance. The obtained polymers possess a hollow microspheric structure, and show moderate hydrogen storage and carbon dioxide uptake capacities.

EXPERIMENTAL SECTION

Materials and Methods. All condensation reactions were operated using standard Schlenk line technique. Anhydrous potassium carbonate, *p*-toluene sulfonic acid, phosphorus oxychloride, *N*,*N*-dimethylformamide, *o*-dichlorobenzene, and tetrahydrofuran were purchased from Beijing chemical reagent company. Triphenylamine, 1,3,5-tribromobenzene, and bis(triphenylphosphine)palladium(II) dichloride were purchased from Aldrich. Tris(4-iodophenyl)amine and 1,3,5-tri(4-bromophenyl)benzene were synthesized according to the reported procedures,[34,35] respectively. The detailed synthesis procedures of tri(4-formylphenyl)amine (**M1**), tri(4-formylbiphenyl)amine (**M2**), 1,3,5-tri(4-formylphenyl)benzene (**M3**), and 1,3,5-tri(4-formylbiphenyl)benzene (**M4**) are included in the Supporting Information. Ethyl acetate, petroleum ether, dichloromethane, acetone, and other chemical reagents were used as received.

Preparation of Benzoin-Based Porous Organic Polymers (BPOPs). A mixture of **M1** (50 mg, 0.15 mmol) and *p*-toluene sulfonic acid was suspended in *o*-dichlorobenzene (4.00 mL). After ultrasonicaion for 0.5 h, the mixture was degassed by at least three freeze–pump–thaw cycles. The tube was frozen at 77 K (liquid nitrogen bath) and evacuated to high vacuum and flame-sealed. After 180 °C for 72 h, the reaction mixture gave a solid in a quantitative yield. This solid was filtrated and washed with acetone, dichloromethane, and ethanol subsequently. The product (denoted **BPOP-1**) was dried in vacuo at 120 °C for more than 12 h.

Similar to the preparation of **BPOP-1**, **M2**, **M3**, and **M4** were used to afford **BPOP-2**, **BPOP-3**, and **BPOP-4** in quantitative yields, respectively.

Scheme 2. Schematic Representation of the Possible Structures of Microporous Organic Networks through Benzoin Condensation (BPOP-1−BPOP-4)

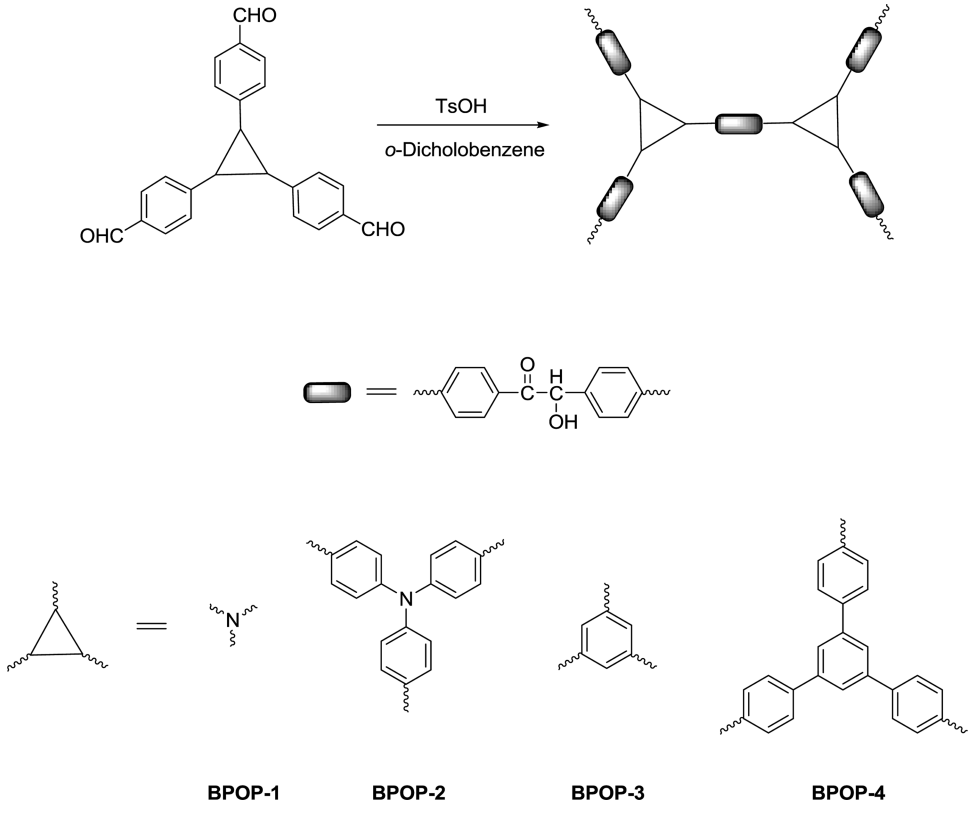

Instrumental Characterization. ^{1}H NMR spectra were recorded on a Bruker DMX400 NMR spectrometer, with tetramethylsilane as an internal reference. Solid-state ^{13}C CP/MAS NMR measurements were performed on a Bruker Avance III 400 spectrometer. Thermogravimetric analysis (TGA) was performed on a Pyris Diamond thermogravimetric/differential thermal analyzer by heating the samples at 10 °C min^{-1} to 800 °C in the atmosphere of nitrogen. Infrared (IR) spectra were recorded in KBr pellets using a Spectrum One Fourier transform infrared (FT-IR) spectrometer (PerkinElmer Instruments Co. Ltd., USA). The sample was prepared by dispersing the polymers in KBr and compressing the mixture to form disks, and 15 scans were signal-averaged. Elemental analysis was obtained on Flash EA 1112 CHN elemental analyzer. Transmission electron microscopy (TEM) observations were carried out using a Tecnai G^2 F20 U-TWIN microscope (FEI, USA) at an accelerating voltage of 200 kV. Energy dispersive X-ray (EDX) detector was used to analyze the chemical elements of the samples. The sample was prepared by dropping an ethanol suspension of **BPOP-1−BPOP-4** onto a copper grid, respectively. Field-emission scanning electron microscopy (SEM) observations were performed on a Hitachi S-4800 microscope (Hitachi Ltd., Japan) operating at an accelerating voltage of 6.0 kV. SEM samples were prepared by dropping an ethanol suspension of **BPOP-1−BPOP-4** on a silicon wafer and left to dry in air. Nitrogen adsorption−desorption and hydrogen adsorption experimentations were conducted using an ASAP 2020 M+C accelerated surface area and porosity analyzer (Micromeritics, USA) at 77 K. Carbon dioxide uptake experimentation was performed by using a TriStar II 3020 surface area and porosity analyzer (Micromeritics, USA) at 273 K. Before measurement, the samples were degassed in vacuo at 120 °C for more than 12 h. Specific surface area was calculated from nitrogen adsorption data by Brunauer−Emmett−Teller (BET) analysis in the relative pressure (P/P_0) range from 0.01 to 0.10 (see the Supporting Information), whereas pore size and pore size distribution were estimated through the original density function theory (DFT). Total pore volume was calculated from nitrogen adsorption−desorption isotherms at P/P_0 = 0.99, whereas micropore volume was calculated from nitrogen adsorption isotherm using the *t*-plot method.

RESULTS AND DISCUSSION

To obtain microporous organic polymers by benzoin condensation, a series of triformyl compounds (**M1−M4**) with either triphenylamine or triphenylbenzene core have been synthesized by formylation of triphenylamine and Suzuki coupling reaction of aromatic halides with formylphenylboronic acid (Figure 1). They can be employed in the one-pot self-condensation approach to produce the α-hydroxyl ketone linked polymers (Scheme 2). It is believed that the self-condensation or self-polymerization is a powerful route to prepare polymers. Only one single monomer is used, and there is no problem with the excess of monomers. The formyl-containing compounds were suspended in *o*-dichlorobenzene, and *p*-toluene sulfonic acid as a catalyst was also added into the reaction system. After self-polymerization in sealed tube at 180 °C for 72 h, four black polymers **BPOP-1−BPOP-4** formed in quantitative yields. In the whole course of preparation, the straightforward generation of **BPOPs** is involved with the use of cheap catalysts and/or reagents, preferably in a metal-free process. Additionally, the catalyst and solvent can be easily removed from the reaction system after the polymerization, just by continuous washing with water and ethanol. Sealed tube polymerization method is often used in the preparation of microporous organic polymers.[12,20] Because of anhydrous oxygen-free condition and high reaction temperature, a polymer that possesses a higher condensation degree and specific surface area can be obtained.[20,24] All the obtained polymers are stable and insoluble in common organic solvents, such as dichloromethane, ethanol, and *N*,*N*-dimethylformamide. The elemental

analysis is utilized to roughly evaluate the degree of condensation of the obtained polymers, and the results are listed in the Table S1 (see the Supporting Information). The content of carbon element is slightly higher than the calculated value, while the content of oxygen element is slightly lower than the calculated value, indicating that a little carbonization might take place in the process of polymerization under *p*-toluene sulfonic acid-catalyzed high-temperature conditions. This kind of carbonization was also observed in the preparation of CTFs.[36,37] Trace amount of sulfur is in the skeleton of the resulting polymers, which is consistent with the EDX results.

Thermal stability of the obtained polymers was investigated by thermogravimetric analysis (Figure 2). The TGA traces

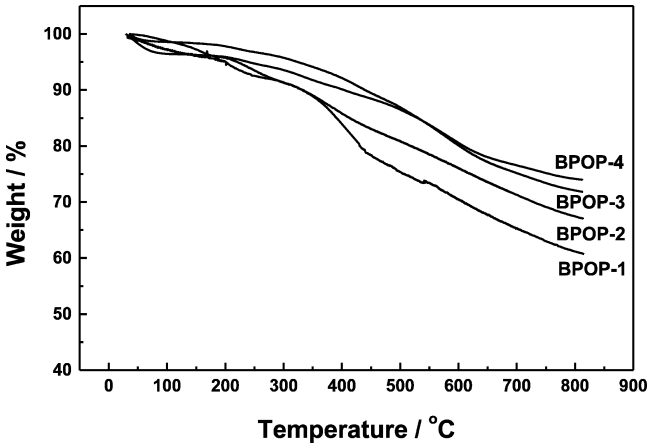

Figure 2. Thermogravimetric analysis (TGA) of **BPOP-1**, **BPOP-2**, **BPOP-3**, and **BPOP-4**.

show that **BPOP-3** and **BPOP-4**, which possess more large conjugated system, have a higher thermal stability than **BPOP-1** and **BPOP-2** containing a triphenylamine core. The thermal decomposition temperature (T_d) is up to ca. 210 °C for **BPOP-1** and **BPOP-2** and ca. 310 °C for **BPOP-3** and **BPOP-4.** With increase in temperature, all the polymers show a continuous mass loss and the residual mass varies from 70% to 60%. The polar α-hydroxyl ketone linkage might be responsible for this continuous mass loss. At higher temperature, further dehydration and condensation of hydroxyl and carbonyl could occur, and the skeletons of polymers were finally damaged.

The obtained α-hydroxyl ketone-linked polymers were confirmed by Fourier transform infrared (FT-IR) spectroscopy. As compared to the spectra of their corresponding monomers, the absorption peaks of all the polymers become weaker (Figure 3 and Figure S1–S3, Supporting Information). Two sharp bands of medium intensity which can be attributed to the C–H stretching vibration of formyl group near 2820 and 2730 cm^{-1} are significantly reduced. Due to the consumption of the half of the carbonyl in benzoin condensation, absorption peak at 1690 cm^{-1} assigned to the stretching vibration of carbonyl is also remarkably reduced. These polymers exhibit a new band at ca. 1030–1050 cm^{-1} for the C–OH stretching vibration, indicative of the presence of the α-hydroxyl ketone linkage. Since the signals of fingerprint region at 700–900 cm^{-1} show no obvious change, the aromatic rings of monomers are preserved in the skeletons of the resultant polymers after condensation.

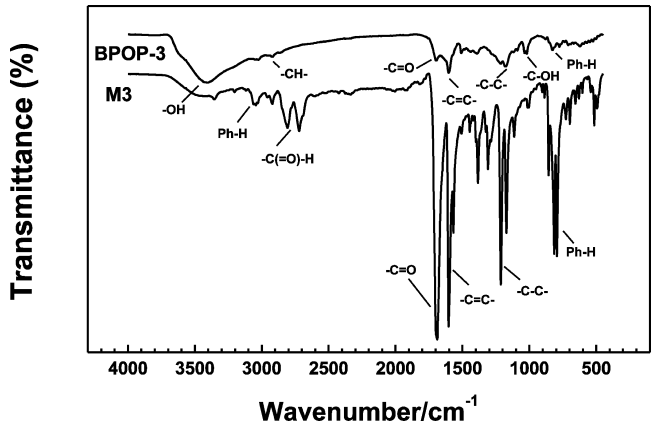

Figure 3. FT-IR spectra of 1,3,5-tri(4-formylphenyl)benzene (**M3**) and **BPOP-3**.

A more detailed analysis of the structure of the obtained polymers was performed by solid-state ^{13}C CP/MAS NMR spectroscopy. The ^{13}C chemical shifts of these polymers are similar to each other. Typically, the spectrum of **BPOP-3** shows two major resonances at 141 and 128 ppm, which can be assigned to the substituted and unsubstituted aromatic carbon atoms, respectively (Figure 4). However, an additional peak

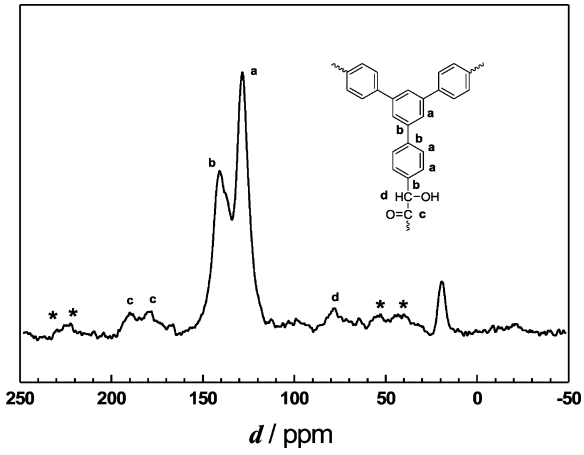

Figure 4. Solid-state ^{13}C CP/MAS NMR spectrum of **BPOP-3** recorded at MAS rate of 5 kHz. Asterisks (*) indicate peaks arising from spinning side bands.

that is the signal of the carbon atoms linked to nitrogen atom appears at the spectra of **BPOP-1** and **BPOP-2** (Figures S4 and S5, Supporting Information). The carbonyl group of α-hydroxyl ketone is observed at 180 ppm, while 188 ppm may be ascribed to the terminal formyl groups. The peak at 78 ppm is also observed for the α-hydroxyl carbon atom. However, the peak at 180 ppm is almost invisible in the spectra of **BPOP-1** and **BPOP-2** (Figures S4 and S5, Supporting Information). It is probable that a little carbonization (Table S1, Supporting Information) results in a low intensity of some peaks at 180 ppm. The resonance at 19 ppm is ascribed to the methyl group of the residue *p*-toluene sulfonic acid, which can not be removed by simple Soxhlet extraction with organic solvents. Energy-dispersive X-ray (EDX) analysis of the obtained polymers is also utilized to evaluate the purity of polymeric phase. It was found that nitrogen element exists in the polymers of **BPOP-1** and **BPOP-2**, and trace sulfur in the skeleton of the

resulting polymers was also detected in EDX index. (Figures S7−S9, Supporting Information)

The morphology of the obtained polymers was investigated by scanning electron microscopy (SEM) and transmission electron microscopy (TEM) measurements. The SEM images reveal regular microspheres of 3.5−5.0 μm for these **BPOP**s (Figure 5). The surfaces of microspheres are not smooth,

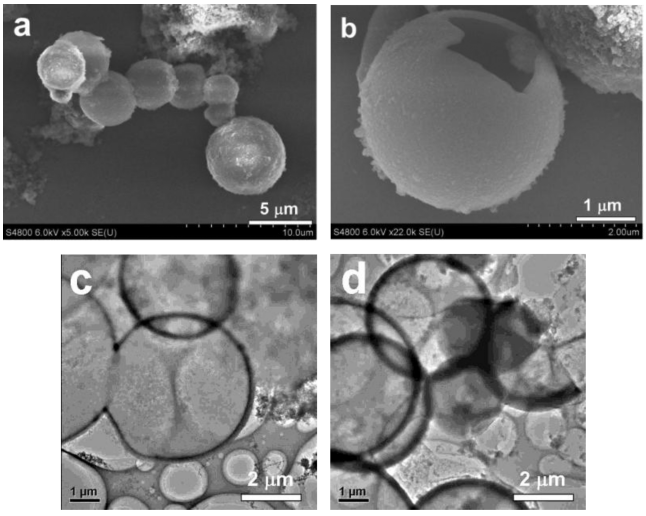

Figure 5. (a, b)SEM and (c, d) TEM images of (a, c) **BPOP-1** and (b, d) **BPOP-3**.

consisting of irregular nanoparticles and nanoplatelets. The high contrast between the dark edges and the bright central part in the TEM images (Figure 5) and some broken spheres in the SEM images (Figure S10, Supporting Information) reveal the hollow nature of the **BPOPs** spheres. The thickness of wall is estimated as 150−200 nm. This kind of hollow structures were also observed in other kinds of polymers such as imidazolium salts-based organic networks[38] and conjugated poly(aryleneethynylene) networks.[9] The Oswald ripening mechanism is prevalently known regarding the template-free formation of hollow structure. In the SEM images, some microspheres with much thicker wall, are observed from the samples (Figure S10, Supporting Information). Thus, our process seems to follow this ripening mechanism.

Nitrogen adsorption−desorption isotherm measurements can analyze the porous properties of microporous networks. Figure 6a shows the nitrogen adsorption−desorption isotherms of **BPOP-1**−**BPOP-3** (Figure S11 for **BPOP-4**, Supporting Information). The isotherms show a high gas uptake at the relative pressure (P/P_0) less than 0.02, a flat course at the middle relative pressure, and a sharp gas adsorption at the high relative pressure, especially for the isotherm of **BPOP-3**, indicating a significant microporosity and macroporosity in the obtained polymers. The presence of macroporous structure can be interpreted as the interparticulate voids arising from the loose packing of some hollow spheres as seen from the SEM images.[39] A little hysteresis of the isotherms is observed, indicative of a little swelling efficiency of the polymer matrix resulted from a high degree of benzoin condensation of our polymers.[2,40] The specific surface area is calculated by employing the Brunauer−Emmet−Teller (BET) approach over different pressure ranges.[41] (Figure S12, Supporting Information) The obtained values, which are comparable with other microporous organic networks,[6] are summarized in the

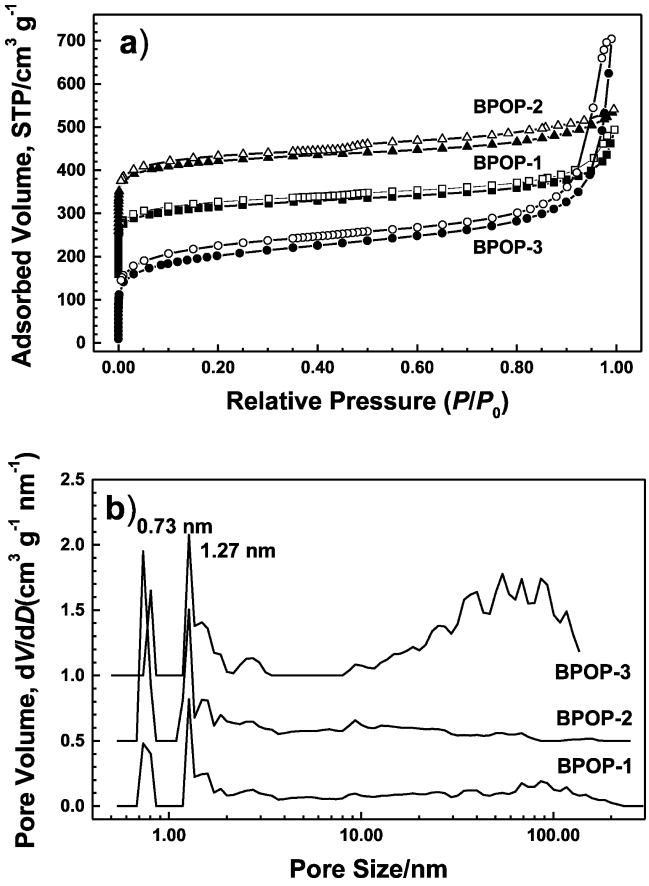

Figure 6. (a) Nitrogen adsorption−desorption isotherms of **BPOP-1** (square), **BPOP-2** (uptriangle), and **BPOP-3** (circle) at 77 K. The isotherms of **BPOP-1** and **BPOP-2** were offset by 100 cm^3 g^{-1} for the purpose of clarity. (b) PSD profiles calculated by the original DFT method. The PSD profiles of **BPOP-2** and **BPOP-3** were offset by 1 unit for the purpose of clarity.

Table 1 and S2. The highest BET specific surface area up to 736 m^2 g^{-1} was obtained for the polymer **BPOP-3** with a total pore volume of 1.09 cm^3 g^{-1} determined at P/P_0 = 0.99. Because of the conformational flexibility of tripod-like structure of triphenylamine unit, the specific surface area of **BPOP-1** and **BPOP-2** is lower than that of **BPOP-3**. However, **BPOP-4** containing the longest monomer strut length possesses the lowest value.[9] As calculated by using original density functional theory (DFT), Figure 6b shows the pore size distribution (PSD) profiles of **BPOP-1**−**BPOP-3**, in which two steep peaks are located at ca. 0.73 and 1.27 nm in the micropore area, whereas the content of the mesopore is little. However, a great amount of macropores can be seen from PSD profile of **BPOP-3**.

The hydrogen and carbon dioxide adsorption properties of the polymers were also investigated by volumetric method (Figure 7 and Table 1). Hydrogen storage capacities for these polymers vary between 1.09 and 1.42 wt % measured at 77 K and 1.0 bar. Abnormally, a relatively high hydrogen uptake value for **BPOP-4** is over expected for polymers with such a low BET specific surface area. It is probable that the polymer **BPOP-4** might have a great amount of ultramicropores which can be accessible by hydrogen, while inaccessible for nitrogen.[42] There is no correlation relationship found between the hydrogen uptake and the BET specific surface area for **BPOP-1**, **BPOP-2**, and **BPOP-3**. Therefore, the other pore

Table 1. Porosity Properties and Gas (hydrogen and carbon dioxide) Uptake of Microporous Polymers BPOPs

polymers	monomers	S_{BET} (m^2 g^{-1})[a]	V_{micro} (cm^3 g^{-1})[b]	V_{total} (cm^3 g^{-1})[c]	CO_2 uptake (wt %)[d]	H_2 uptake (wt %)[e]
BPOP-1	**M1**	664	0.15	0.55	15.3	1.09
BPOP-2	**M2**	632	0.15	0.45	8.94	1.42
BPOP-3	**M3**	736	0.14	1.09	11.7	1.33
BPOP-4	**M4**	268	0.02	0.11	8.03	1.20

[a]Surface area calculated from the nitrogen adsorption isotherm using the BET approach in the relative pressure (P/P_0) range from 0.01 to 0.10. [b]Micropore volume calculated from nitrogen adsorption isotherm using the t-plot method. [c]Total pore volume at P/P_0 = 0.99. [d]Carbon dioxide gravimetric uptake capacities at 273 K. [e]Hydrogen gravimetric uptake capacities at 77 K measured at hydrogen equilibrium pressure of 1.0 bar.

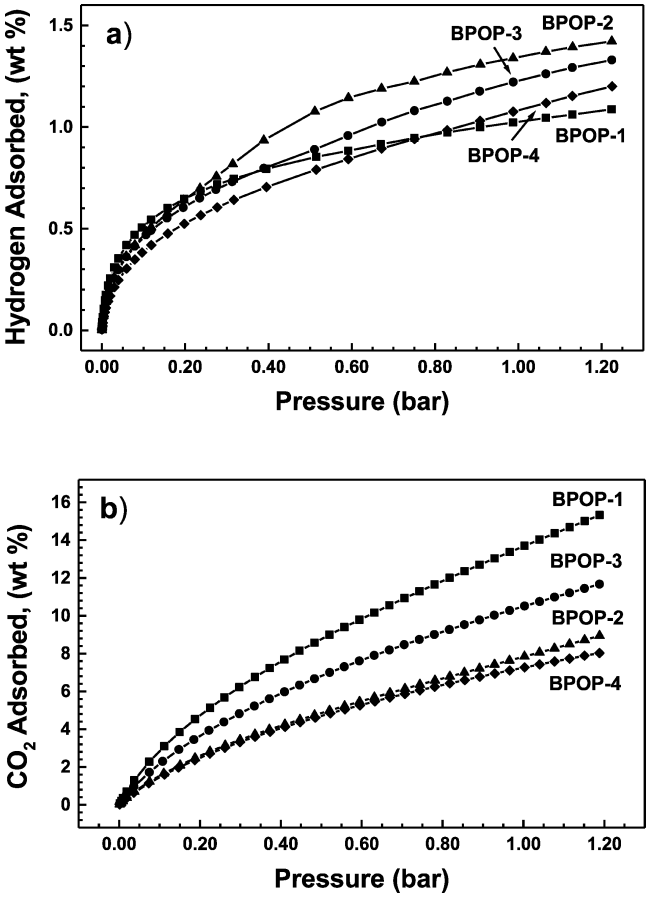

Figure 7. (a) Gravimetric hydrogen and (b) carbon dioxide adsorption isotherms for **BPOP-1** (square), **BPOP-2** (uptriangle), **BPOP-3** (circle), **BPOP-4** (diamond) at 77 K and 273 K, respectively.

parameters (pore size, pore volume, and pore size distribution), polar linkage (α-hydroxyl ketone) and heteroatom (nitrogen) are important factors to the determination of the hydrogen sorption performance. The adsorption isotherms for the polymers **BPOP-1** and **BPOP-3** show a rather high capacity for carbon dioxide, 15.3 wt % (78 cm^3 g^{-1}, STP) and 11.7 wt % (59 cm^3 g^{-1}, STP), even though **BPOP-1** possesses a lower specific surface area than that of **BPOP-3**. This adsorption amount of our polymers has exceeded some metal−organic frameworks[43] and zeolitic imidazolate frameworks.[44] The nitrogen atoms in the polymeric skeleton should play an important role in determining carbon dioxide uptake.[23] The high charge density at the nitrogen sites can facilitate local-dipole−quadrupole interactions with carbon dioxide.[45] However, carbon dioxide capacity for **BPOP-2** that possesses a similar specific surface area to **BPOP-1** is much lower. The porosity properties of microporous networks are also a crucial factor.

CONCLUSION

In summary, we have demonstrated a facile approach to prepare microporous organic networks through benzoin condensation. This reaction was used to synthesize nanoporous polymers for the first time on the basis of the self-condensation of multiformyl-containing monomers. Four α-hydroxyl ketone linked polymers were obtained, and they possess modest BET specific surface area up to 736 m^2 g^{-1}. FT-IR and solid-state ^{13}C CP/MAS NMR spectroscopy confirm the α-hydroxyl ketone linkage of the obtained polymers. From the SEM and TEM images, the hollow microspheric morphology can be observed. Gas adsorption investigation shows that the obtained polymers possess a moderate hydrogen capacity and carbon dioxide uptake. These excellent performances would make our polymers become promising materials for gas storage.

ASSOCIATED CONTENT

Supporting Information

Details of synthesis of monomers, element analysis, FT-IR data, solid-state ^{13}C CP/MAS NMR spectra, EDX spectra, SEM images, and BET surface areas plot data. This material is available free of charge via Internet at http://pubs.acs.org.

AUTHOR INFORMATION

Corresponding Author

*Tel: +86 10 8254 5576. E-mail: hanbh@nanoctr.cn.

Notes

The authors declare no competing financial interest.

ACKNOWLEDGMENTS

The financial support of the National Science Foundation of China (Grants 91023001 and 61261130092), the Ministry of Science and Technology of China (National Major Scientific Research Program, Grant 2011CB932500), and the Chinese Academy of Sciences (Knowledge Innovation Program, Grant KJCX2-YW-H21) is acknowledged.

REFERENCES

(1) Hasell, T.; Wood, C. D.; Clowes, R.; Jones, J. T. A.; Khimyak, Y. Z.; Adams, D. J.; Cooper, A. I. *Chem. Mater.* **2010**, *22*, 557−564.
(2) Mckeown, N. B.; Budd, P. M.; Msayib, K. J.; Ghanem, B. S.; Kingston, H. J.; Tattershall, C. E.; Makhseed, S.; Reynolds, K. J.; Fritsch, D. *Chem.−Eur., J.* **2005**, *11*, 2610−2620.
(3) Weber, J.; Thomas, A. *J. Am. Chem. Soc.* **2008**, *130*, 6334−6335.
(4) Thomas, A. *Angew. Chem., Int. Ed.* **2010**, *49*, 8328−8344.
(5) Cooper, A. I. *Adv. Mater.* **2009**, *20*, 1291−1295.
(6) McKeown, N. B.; Budd, P. M. *Macromolecules* **2010**, *43*, 5163−5176.

(7) Budd, P. M.; Ghanem, B. S.; Makhseed, S.; Mckeown, N. B.; Msayib, K. J.; Tattershall, C. E. *Chem. Commun.* **2004**, *40*, 230−231.
(8) Jiang, J.-X.; Su, F.; Niu, H.; Wood, C. D.; Campbell, N. L.; Khimyak, Y. Z.; Cooper, A. I. *Chem. Commun.* **2008**, *44*, 486−488.
(9) Jiang, J.-X.; Su, F.; Trewin, A.; Wood, C. D.; Campbell, N. L.; Niu, H.; Dickinson, C.; Ganin, A. Y.; Rosseinsky, M. J.; Khimyak, Y. Z.; Cooper, A. I. *Angew. Chem., Int. Ed.* **2007**, *46*, 8574−8578.
(10) Schmidt, J.; Werner, M.; Thomas. *Macromolecules* **2009**, *42*, 4426−4429.
(11) Furukawa, H.; Yaghi, O. M. *J. Am. Chem. Soc.* **2009**, *131*, 8875−8883.
(12) Kuhn, P.; Thomas, A.; Antonietti, M. *Macromolecules* **2009**, *42*, 319−326.
(13) Chen, Q.; Wang, J.-X.; Yang, F.; Zhou, D.; Bian, N.; Zhang, X.-J.; Yan, C.-G.; Han, B.-H. *J. Mater. Chem.* **2011**, *21*, 13554−13560.
(14) Chen, Q.; Wang, T.; Wang, J.-X.; Zhou, D.; Han, Y.; Zhang, C.-S.; Yan, C.-G.; Han, B.-H. *Macromolecules* **2011**, *44*, 5573−5577.
(15) Chen, Q.; Wang, Q.; Luo, M.; Mao, L.-J.; Yan, C.-G.; Li, Z.-H.; Han, B.-H. *Polymer* **2012**, *53*, 2032−2037.
(16) Vile, J.; Carta, M.; Bezzu, C. G.; McKeown, N. B. *Polym. Chem.* **2011**, *2*, 2257−2260.
(17) Hashem, M.; Bezzu, C. G.; Kariuki, B. M.; McKeown, N. B. *Polym. Chem.* **2011**, *2*, 2190−2192.
(18) Schwab, M. G.; Fassbender, B.; Spiess, H. W.; Thomas, A.; Feng, X.; Müllen, K. *J. Am. Chem. Soc.* **2009**, *131*, 7216−7217.
(19) Zhao, Y.-C.; Zhou, D.; Chen, Q.; Zhang, X.-J.; Bian, N.; Qi, A.-D.; Han, B.-H. *Macromolecules* **2011**, *44*, 6382−6388.
(20) Uribe-Romo, F. J.; Doonan, C. J.; Furukawa, H.; Oisaki, K.; Yaghi, O. M. *J. Am. Chem. Soc.* **2011**, *133*, 11478−11481.
(21) Reich, T. E.; Jackson, K. T.; Li, S.; Jena, P.; Ei-Kaderi, H. M. *J. Mater. Chem.* **2011**, *21*, 10629−10632.
(22) Rabbani, M. G.; El-Kaderi, H. M. *Chem. Mater.* **2011**, *23*, 1650−1653.
(23) Zhao, Y.-C.; Cheng, Q.-Y.; Zhou, D.; Wang, T.; Han, B.-H. *J. Mater. Chem.* **2012**, *22*, 11509−11514.
(24) Li, B.; Gong, R.; Wang, W.; Huang, X.; Zhang, W.; Li, H.; Hu, C.; Tan, B. *Macromolecules* **2011**, *44*, 2410−2414.
(25) Chen, Q.; Min, L.; Hammershøj, P.; Zhou, D.; Han, Y.; Laursen, B. W.; Yan, C.-G.; Han, B.-H. *J. Am. Chem. Soc.* **2012**, *134*, 6084−6087.
(26) Wu, D.; Xu, F.; Sun, B.; Fu, R.; He, H.; Matyjaszewski, K. *Chem. Rev.* **2012**, *112*, 3959−4015.
(27) Yuan, D.; Lu, W.; Zhao, D.; Zhou, H.-C. *Adv. Mater.* **2011**, *23*, 3723−3725.
(28) Baragwanath, L.; Rose, C. A.; Zeitler, K.; Connon, S. J. *J. Org. Chem.* **2009**, *74*, 9214−9217.
(29) Yuan, S.; Dorney, B.; White, D.; Kirklin, S.; Zapol, P.; Yu, L.; Liu, D.-J. *Chem. Commun.* **2010**, *46*, 4547−4549.
(30) Yuan, S.; Kirklin, S.; Dorney, B.; Liu, D.-J.; Yu, L. *Macromolecules* **2009**, *42*, 1554−1559.
(31) Holst, J. R.; Stöckel, E.; Adams, D. J.; Cooper, A. I. *Macromolecules* **2010**, *43*, 8531−8538.
(32) Kuhn, P.; Antonietti, M.; Thomas, A. *Angew. Chem., Int. Ed.* **2008**, *47*, 3450−3453.
(33) Ren, H.; Ben, T.; Wang, E.; Jing, X.; Xue, M.; Liu, B.; Cui, Y.; Qiu, S.; Zhu, G. *Chem. Commun.* **2010**, *46*, 291−293.
(34) Ning, Z.; Chen, Z.; Zhang, Q.; Yan, Y.; Qian, S.; Cao, Y.; Tian, H. *Adv. Funct. Mater.* **2007**, *17*, 3799−3807.
(35) Elmorsy, S. S.; Pelter, A.; Smith, K. *Tetrahedron Lett.* **1991**, *32*, 4175−4176.
(36) Bojdys, M. J.; Jeromenok, J.; Thomas, A.; Antonietti, M. *Adv. Mater.* **2010**, *22*, 2202−2205.
(37) Dawson, R.; Cooper, A. I.; Adams, D. J. *Prog. Polym. Sci.* **2012**, *37*, 530−563.
(38) Cho, H. C.; Lee, H. S.; Chun, J.; Lee, S. M.; Kim, H. J.; Son, S. U. *Chem. Commun.* **2011**, *47*, 917−919.
(39) Yu, H.; Shen, C.; Tian, M.; Qu, J.; Wang, Z. *Macromolecules* **2012**, *45*, 5140−5150.
(40) Weber, J.; Schmidt, J.; Thomas, A.; Böhimann, W. *Langmuir* **2010**, *26*, 15650−15656.
(41) Dawson, R.; Laybourn, A.; Clowes, R.; Khimyak, Y. Z.; Adams, D. J.; Cooper, A. I. *Macromolecules* **2009**, *42*, 8809−8816.
(42) Zhang, B.; Zhang, Z. *Chem. Commun.* **2009**, *45*, 5027−5029.
(43) Choi, S. B.; Seo, M. J.; Cho, M.; Kim, Y.; Jin, M. K.; Jung, D.-Y.; Choi, J.-S.; Ahn, W.-S.; Rowsell, J. L. C.; Kim, J. *Cryst. Growth Des.* **2007**, *7*, 2290−2293.
(44) Banerjee, R.; Phan, A.; Wang, B.; Knobler, C.; Furukawa, H.; O'Keeffe, M.; Yaghi, O. M. *Science* **2008**, *319*, 939−943.
(45) Farha, O. K.; Spokoyny, A. M.; Hauser, B. G.; Bae, Y.-S.; Brown, S. E.; Snurr, R. Q.; Mirkin, C. A.; Hupp, J. T. *Chem. Mater.* **2009**, *21*, 3303−3305.